Multilayer injection molding

E. Vos, H. E. H. Meijer and G. W. M. Peters*
Department of Mechanical Engineering, Eindhoven University of Technology, Eindhoven, The Netherlands

Multilayer Injection Molding

Visualization of the fountain flow in a piston driven non-Newtonian flow is studied by means of experiments and numerical computation. The result will be applied to the multilayer injection molding technique, where an accumulator is used, to store the polymer melt. The discontinuity at the contactline of the piston and the wall of the cylinder appears to have considerable influence on the total deformation history.

1 Introduction

Using a multicomponent injection molding technique layered structures of two or more materials can be realized within thin-walled products. Depending on the position of the gate (mostly centergated), the geometry of the nozzle (mostly concentric cylinders) and the method of injection (A, B; A, B, A; A, A/B, A; A, B/A, A; A, B/A/B, A; etc.) thin or thick, centric or excentric layers can be realised in the product (see Fig. 1). The technology differs from multicolor injection molding (e.g. rear-lights of cars, keys of typewriters), where a first part of the product is transferred into a larger mold and where the second material is injected against or around this part.

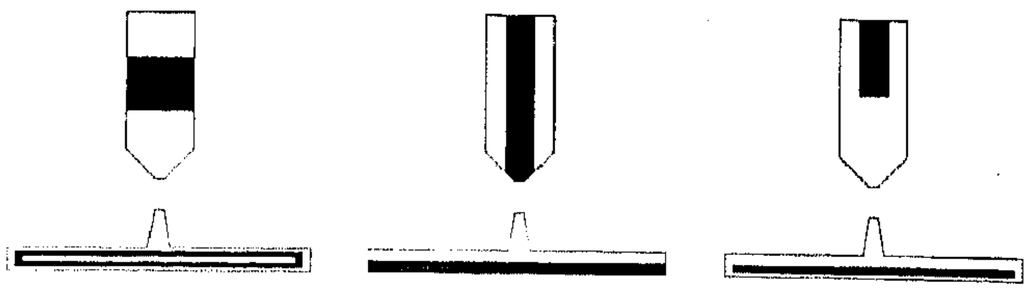

Fig. 1. Two component injection molding with sequential, simultaneous and combined injection

The multicomponent technology as such is not very new: introduced in 1967 by ICI it promised to be a breakthrough in the manufacturing of stiff, large and light-weight products. Applications in practice are however restricted to sandwich constructions, where, via a sequential injection (A, B; A, B, A), three layers in the product are realized. The material of the inner layer B typically consists of the A material, containing a physical or chemical foaming agent. Sandwich-products with hard, flat and glossy outer layers and a light, foamed inner layer looked rather promising in the automotive, housing and sanitary branches, since large parts could be molded without the need of large machines with high clamping forces, since shrinkage during cooling is compensated for by expansion of the foam rather than by packing at high pressures. The natural limitations of the process (minimum density of the foam: 300 kg/m³, ratio A/B: 50/50, with non-uniform layer thickness) reduces however the applications to products where, for other reasons (e.g. esthetic) thick walls are preferred, since light-weight, high-stiffness products can be made more economically using ribs.

During the last years experiments have shown that also in thin-walled products this technology is applied. If an adapted method of injection (e.g. A, A/B, A; A, B/A, A) is used thin, excentric layers can be realized with rather uniform thickness over the complete product. This can be of importance for other applications than improving the stiff-

Nomenclature

$A_{1,2}$	constant in Eq. 3, 4	K
B_1	consistency index in Eq. 3, 4	$Pa \cdot s^n$
B_2	consistency index in Eq. 4	
D	diameter of the cylinder	m
$\underline{f}$	body force	$N \cdot kg^{-1}$
F	force	N
L	length of the cylinder	m
n	power-law index	
n	model index	
r	coordinate in radial direction	m
R	radius of the cylinder	m
Re	Reynolds number	
T	temperature	K
$\underline{u}$	velocity vector	$m \cdot s^{-1}$
v	velocity vector component	$m \cdot s^{-1}$
V_p	velocity of the piston	$m \cdot s^{-1}$
z	coordinate in axial direction	m
Subscripts		
b	Bingham	
g	gravity	
p	pressure	
pl	power-law	
r	radial vector component	
z	axial vector component	
Greek letters		
$\dot{\gamma}$	shear rate	s^{-1}
η	viscosity	$Pa \cdot s$
λ	penalty function parameter	$Pa \cdot s$
ρ	density	$kg \cdot m^{-3}$
τ_y	yield stress	$N \cdot m^2$
Symbols		
∇	gradient operator	m^{-1}
Δ	Laplace operator (∇^2)	m^{-2}

* Mail address: Dr. H. E. H. Meijer, Department of Mechanical Engineering, Eindhoven University of Technology, P.O. Box 513, 5600 MB Eindhoven, The Netherlands.

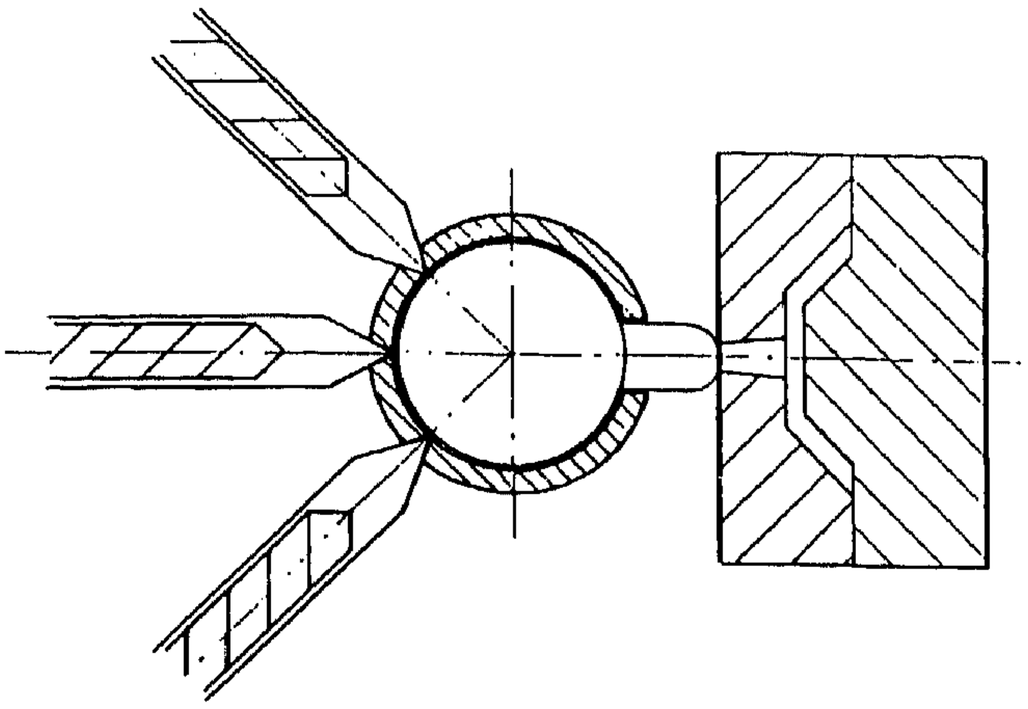

Fig. 2. Three component injection molding

ness pro weight ratio or disposing regrind. Examples are electro-magnetic shielding, where a conductive layer inside the wall of the product is used to create a Faraday-cage or in barrier products, where the thin layer has an extreme low permeability for gases, while the outer layers protect against water and provide the mechanical properties of the product. Some drawbacks of the existing technology should, however, be overcome. The first is the limitation to two materials only. If, as a comparison, coextrusion techniques in profile-extrusion, casting, film- or bottle-blowing should have been restricted to two materials only, these developments would not have been so pronounced, since attractive combinations of polar and apolar materials would have been impossible (the third type material, typically a modified apolar polymer with functional polar groups, acts as a 'glue' layer between both other materials). This drawback is now being removed by the development of a practical three component injection molding technique at our laboratory (Fig. 2). Secondly, the restriction to simple geometries is limiting the number of possible applications, whereas one of the big advantages of the injection molding process is its relative versatility in the geometrical design of products. This drawback can be overcome by the application of (computer) models which can precisely predict where a particle will flow in a mold. The advantage of mathematical models is that they can be inverted: where does a particle have to start, when its final position inside the product is defined. So even in complex geometries one can predict what had to be injected in order to form a specific (e.g. excentric) layer.

Apart from these practical applications, the multicomponent injection technology can be used in order to produce direct tests on the quality of computer models, which describe the injection phase of the process (transient, non-isothermal, 3D-flow of non-Newtonian liquids). The total deformation history of every particle can be investigated, which is also of importance for the calculation of transient viscoelastic stresses, caused by the fast injection, which are partly relaxing and partly frozen in. These stresses are important for predicting the influence of material properties and process-conditions on product quality like precision injection molding, birefringence free molding, stress free molding or the opposite: optimizing the anisotropic mechanical properties, e.g. with the use of liquid chrystalline polymers.

2 Piston driven flow

The development of the multicomponent injection technology will be realized in a number of steps. The first step is the formation of the requested layers during the (short) injection phase. Using this method only simple geometries can be used, because the time required to compose the configuration of the layers is limited by the finite opening and closing times of the valves of the distribution device, while on the other hand injection molding requires a high injection-rate. The second step aims to the possibility of complicated geometries as well, by using an accumulator between the distribution device and the mold. The configuration requested can then be composed during the cooling of the previous product, which increases the time available considerably. After demolding the contents of the accumulator can be injected at one stroke into the mold at a high rate.

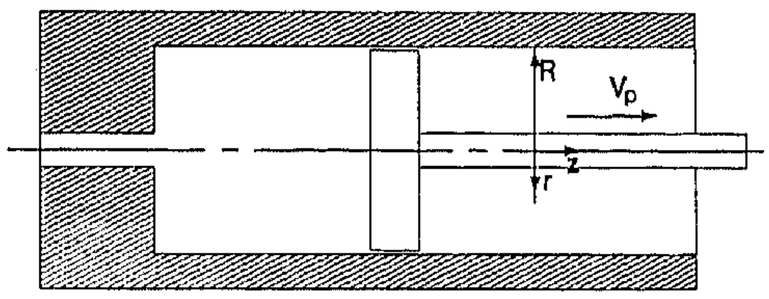

Fig. 3. Basic design of an accumulator

The basic design of the accumulator consists of a piston in a cylinder (Fig. 3). In this study it is investigated to what extent the configuration of the original flow is disturbed by this way of storage. For a minimal disturbance it would be useful if the streamlines for filling and emptying the accumulator are similar (only the velocities have an opposite sign and differ in magnitude). In the region where the flow is basically two-dimensional (and rotatory symmetric) no severe problems are expected, however near the piston a three-dimensional (be it symmetrical) flowfield exists. This complex flow arises from the stick-boundary condition at the piston. It changes with increasing distance from this piston until a fully developed velocity distribution is reached (if allowed by the geometry, L/D, of the accumulator). Only a few investigations have been dedicated to piston driven flow, especially for low Reynolds numbers. Wagner [1] proposed a numerical solution for the transition from plug flow to tube flow and Gerrard [2, 3] studied the time dependence of a flow started from rest by motion of the piston, however he used Reynolds numbers over 400. Our experiments can also be compared with the case of a planar flow with both walls moving at the same velocity.

One of the most extensive theoretical and experimental studies on planar flows, with combined moving and stationary walls, has been performed by Ottino et al. [4, 5, or 31], albeit with a different purpose. They study chaotic mixing in laminair, low Reynolds number flows and use model

liquids. It has been recognized that fluid particles entering the region near the piston decelerate in the direction of flow and acquire a transverse velocity, spilling outwards towards the wall. Exactly this same definition is used to describe the phenomenon which is commonly known as fountain flow (Rose [6]). Although the theory on the 'classical' fountain flow as referred to in literature generally deals with a fluid-flow interface or a free surface, a qualitative contemplation for a fluid-solid interface will follow the same reasoning. Since the introduction of the term 'fountain flow' by Rose [6] several researchers have investigated different aspects of this phenomenon. The general in- or outward movement near a fluid-fluid interface, has been visualized – by White and Dee [7], Dussan [8] and Brown [9] by means of dye markers. Ottino et al. [4, 5] use a similar technique for a fluid-solid interface. Experiments with tracers, giving a more detailed view on the deformation of the fluid through the (free) front region, were performed by Schmidt [10], Cogos, Huang and Schmidt [11] and Coyle et al. [12], the latter gives an extensive description of the phenomenon.

The first attempt to reach an analytical solution of the Navier-Stokes equations was made by Bhattacharji and Savic [13], which resulted in a simplified, but compact solution. Although they solved the problem for a fluid-fluid interface, the solution for a fluid-solid interface was pointed out as well. Hocking [14] derived an equation for an interface of two fluids, which can be applied to a fluid-solid interface. In several studies of mold filling behavior attention has been paid to the fountain flow, having a large influence on the molecular orientation in the injection molded product close to the wall. In these studies numerical solutions of the velocity field in the flow front have been developed, some based on a finite difference method using the Marker-and-Cell technique, see e.g. Kamal and Lafleur et al. [15, 16, 17] and Cogos, Huang and Schmidt [11], some based on a finite element method using the Galerkin formulation, also used in this investigation, see e.g. Lowndes [18], Behrens et al. [19], Coyle et al. [12] or Mavridis et al. [20, 21]. All these investigations have dealt with the problem of a fluid-fluid interface or a free front advancing in a capillary tube or in between plates. Therefore the quantitative solution can not be applied to a piston driven flow,

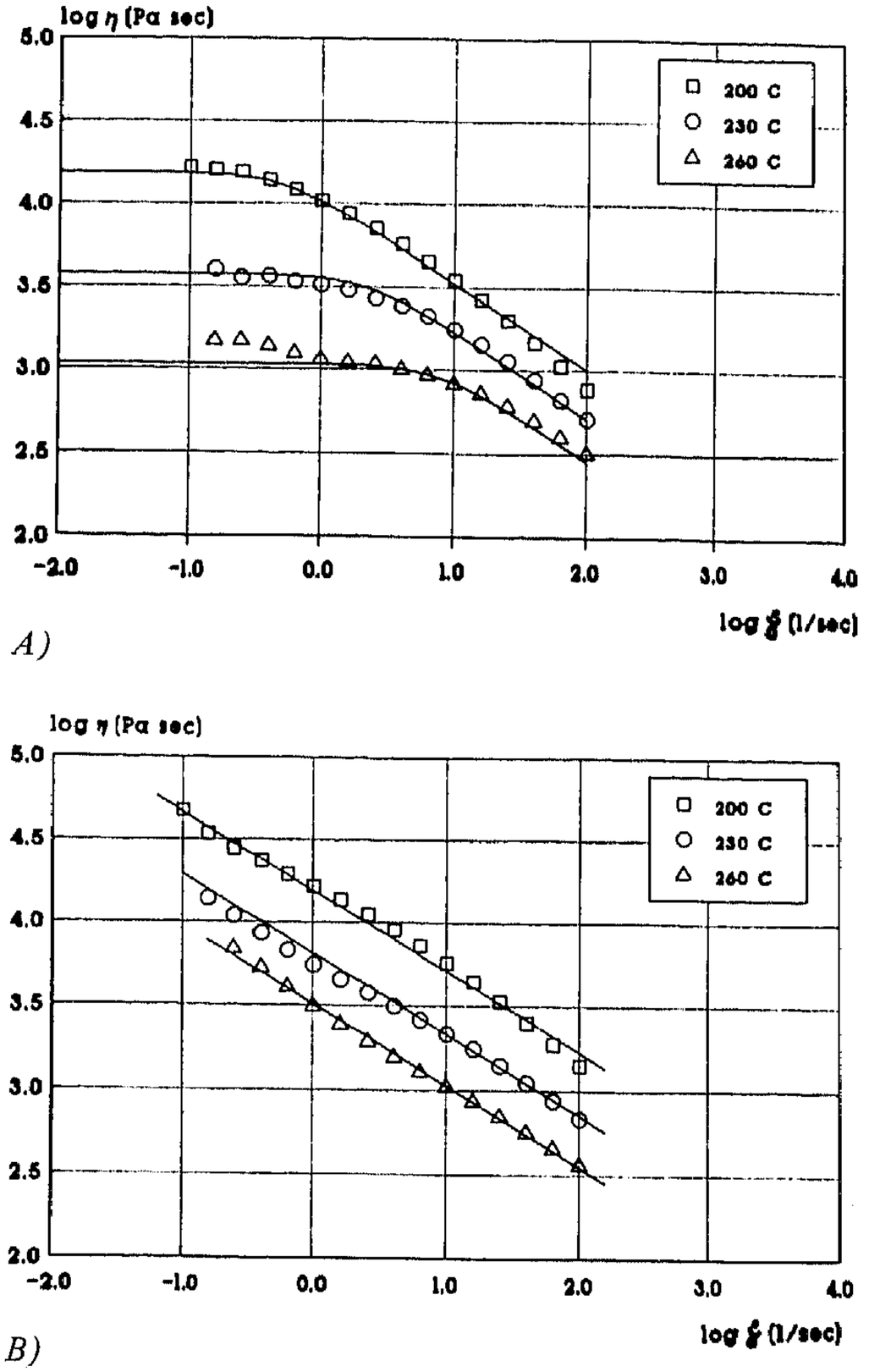

Fig. 5. Flow curves (symbols) with model fits (lines) A: Polystyrene, Eq. 4, B: ABS, Eq. 3

because of the difference in boundary conditions at the piston surface. Nevertheless the qualitative analysis of the effects occuring provides a tool in getting the right picture of the phenomena.

3 Experimental

To simulate the fountain flow, when the piston is driven by the fluid and the reverse fountain flow, when the piston is driving the fluid, a simple but effective apparatus has been developed, schematically shown in Fig. 4. A plug (ϕ 16 mm × 60 mm) consisting of different layers of colored slices is placed in the cylinder and locked up between the two pistons. After the apparatus has been heated, piston 1 is driven upwards at a constant rate by hydraulic pressure (F_p). A weight (F_g) is placed on top of piston 2 to make sure that no slip occurs at the surface of this piston (by air-inclusion). The phenomena occuring at the driven piston at this stage represent the filling of the accumulator. Emptying the accumulator can be simulated by rotating the cylinder over 180°. So piston 2 takes the place of piston 1 and will become the driving piston.

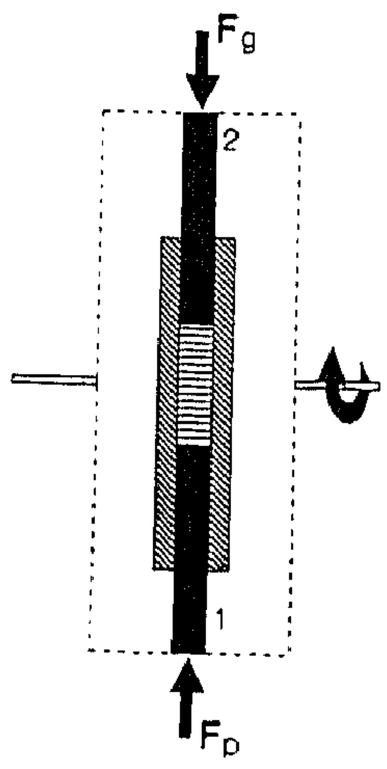

Fig. 4. Experimental set up

The advantage of this set-up is that tracers can be exactly positioned in their solid phase and only become a fluid after melting. The materials used are Polystyrene (PS 634, Dow), showing Newtonian behavior at low shear rates and ABS (Ronfalin FX50, DSM) with a more complex flow behavior at low shear-rates. Flow curves of both materials and their model fits are shown in Fig. 5. The experiments to examine the deformation were performed at 230 °C at two different piston speeds (1.2 and 60 mm/s). Some complementary experiments were carried out to examine the effect of the temperature.

4 Experimental results

When the pressure is activated and piston 1 is driving both, the material and piston 2 upwards, three phenomena occur: a reverse fountain flow near piston 1, a fountain flow near piston 2, and a circular symmetric two dimensional flow in the remaining region. The deformation is visualized using slices of different colors, as shown in Figs. 6 and 7. After different displacements of the piston samples are frozen to investigate the development of the deformation. The displacement of 0 mm shows the effect of heating and cooling only.

In Fig. 6 the results of the deformation are shown for Polystyrene. Dark spots on the photographs, which are not in agreement with the deformation pattern, are shrinkage cavities. From the photographs of Fig. 6 it can be concluded that at the surface of the piston some material remains, forming a continuously thinning layered structure. Once material is entering the fountain flow it moves through the front towards the wall, undergoes some extensional flow and acquires a reverse velocity causing a continuously stretching Z or S-shape. At the driving piston a similar behavior occurs, but here the material is moving inwards. This also results in forming a Z or S-shape, but more towards the centre of the plug.

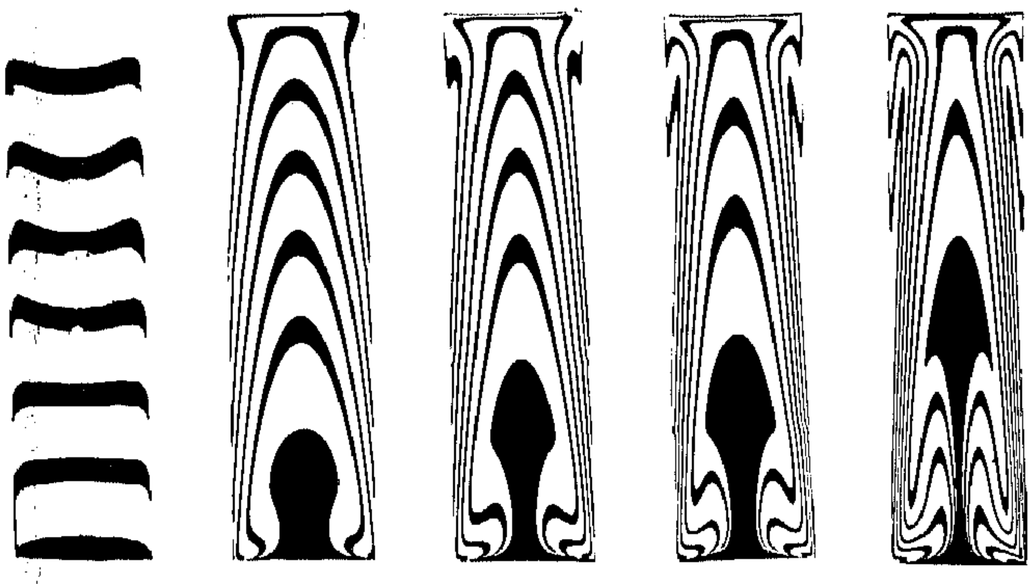

Fig. 6. Deformation of Polystyrene at different piston displacements: 0, 22, 33, 44 and 55 mm respectively

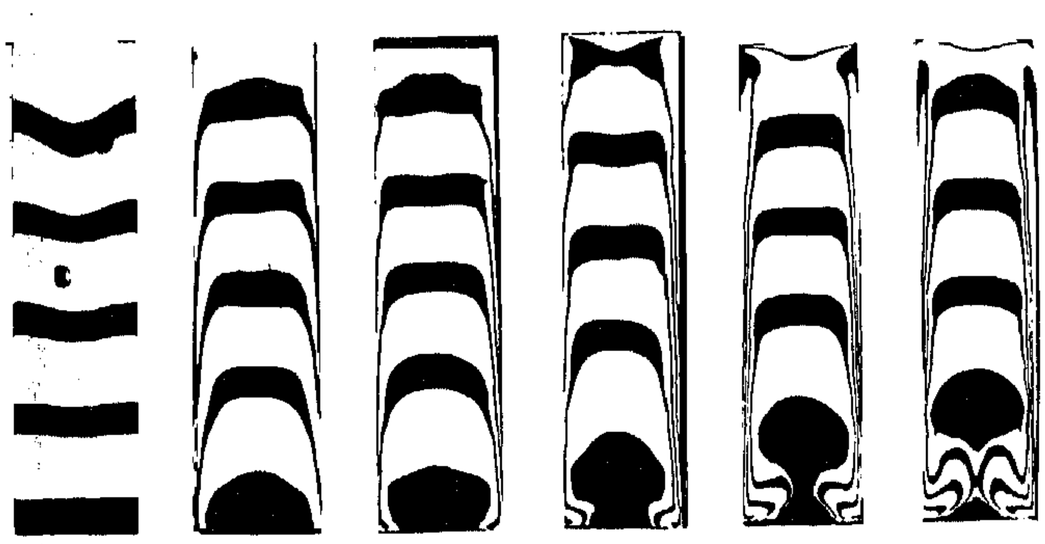

Fig. 7. Deformation of ABS at different piston displacements: 0, 11, 22, 33, 44 and 55 mm

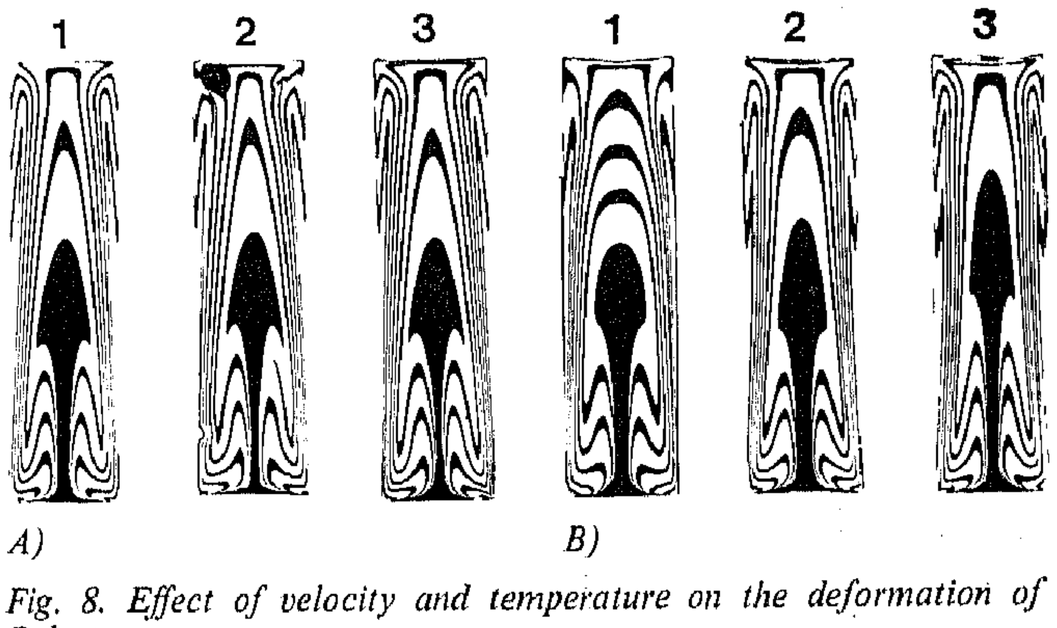

Fig. 8. Effect of velocity and temperature on the deformation of Polystyrene
Velocities: A: 1.2 mm/s B: 60 mm/s, Temperatures: 1: 200 °C, 2: 230 °C 3: 260 °C

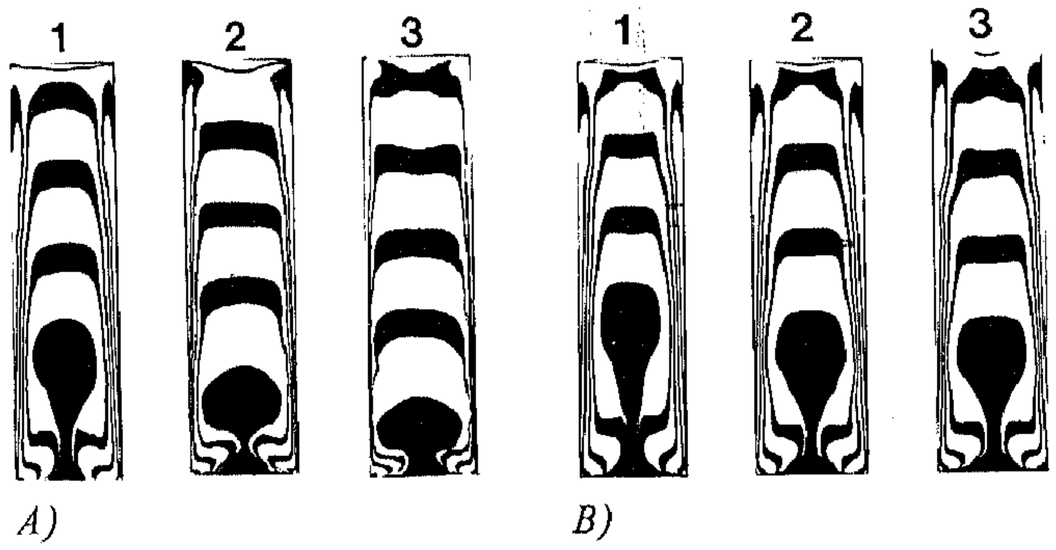

Fig. 9. Effect of velocity and temperature on the deformation of ABS (Velocities and temperatures see Fig. 8)

The results of the experiments using ABS are shown in Fig. 7 and expose a similar behavior forming the Z or S-shapes in the tracers, in spite of the large differences in the velocity profile. This was to be expected because these Z or S-shapes have been proved to appear irrespectively of the rheology of the fluid, see Beris [22] (a response on the work of Mavridis et al. [21]). The shape of the velocity profile varies for different materials or experimental conditions and is expressed in the variety of Z or S-shapes observed. Six different experiments have been performed for both materials, to get an impression of the influence of velocity and temperature on the deformation.

For Polystyrene the results are shown in Fig. 8. It appears that for the low velocity the deformation of the plug is similar at all three temperatures from which it can be concluded that the material behaves like a Newtonian fluid. At the higher speed a non-Newtonian behavior is observed, demonstrated by less developed velocity profiles and unequal deformations at different temperatures. This was to be expected from the flow curves measured. For ABS a plug flow can be observed under all conditions pointing to a non-Newtonian behavior (Fig. 9) and the influence of the temperature at different speeds is almost

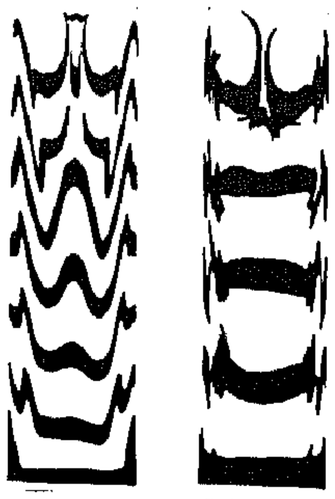

A) B)

Fig. 10. Piston displacement 55 mm up and down for Polystyrene (A) and ABS (B)

opposite as compared to the PS case. An explanation for these facts must result from numerical simulations.

Finally, the piston is moved 55 mm upwards, simulating the filling of the accumulator. After rotating the cylinder 180° the other piston is moved 55 mm, so the reverse movement of the particles is accomplished. The results are shown in Fig. 10. It is to be noticed that the original configuration, a layered structure, is not recovered completely. This means that the complex velocity field near the driving piston is not similar to that at the driven piston.

4.1 Numerical

The velocity field is calculated using the finite element method, based on the Galerkin approach. The flow is considered two-dimensional, incompressible, steady and isothermal. The continuity and Navier-Stokes equations read:

$$\left.\begin{aligned} &\nabla \cdot \underline{u} = 0, \\ &-\eta\, \Delta \underline{u} + \varrho(\underline{u} \cdot \nabla)\underline{u} + \nabla p = \varrho \underline{f}. \end{aligned}\right\} \tag{1}$$

It should be noted that time effects are not included because of the steady-state assumption. The penalty function formulation is used, resulting in the following equations describing the problem:

$$\left.\begin{aligned} &p = -\lambda \nabla \cdot \underline{u} \\ &-(\mu + \lambda)\Delta \underline{u} + \varrho(\underline{u} \cdot \nabla)\underline{u} = \varrho \underline{f}. \end{aligned}\right\} \tag{2}$$

If λ is selected sufficiently large, the solution of $\underline{u}$ and p from Eq. 2 differs negligibly from the exact solution from Eq. 1. The practical advantage of using the penalty function formulation, is that the pressure field is eliminated, resulting in less equations and therefore a more economical computation.

Solving each problem starts with the Newtonian solution for the Stokes equation, next the Newton-Raphson iteration method provides a good solution for the non-Newtonian case or the Navier-Stokes equations in which convective terms are included (Carey and Krishnan [23]).

Two different constitutive equations are used to describe the flow behavior of the materials:

Power-law model

$$\eta = B_1 e^{(A_1/T)} \dot{\gamma}^{n-1}, \tag{3}$$

Carreau model

$$\eta = B_1 e^{(A_1/T)} (1 + (B_2 e^{(A_2/T)} \dot{\gamma})^2)^{\frac{n-1}{2}}. \tag{4}$$

The flow curves in Fig. 5 show that the Power-law model should be most suitable for ABS and the Carreau model for Polystyrene. Fitted values obtained for the parameters of the models are given in Table 1. The flow geometry and the mesh are depicted in Fig. 11. It is assumed that the wall is moving instead of the pistons (compare also the geometry used by Ottino et al. [4]). This causes no essential changes in the problem, but is merely a matter of comfort. On all boundaries, the wall and the pistons, no slip is assumed. The

Table 1. Model parameters

	ABS	Polystyrene
n	0.52	0.48
A_1	$6.56 \cdot 10^3$	$11.13 \cdot 10^3$
B_1	$1.48 \cdot 10^{-2}$	$9.23 \cdot 10^{-7}$
A_2		$11.39 \cdot 10^3$
B_2		$6.69 \cdot 10^{-11}$

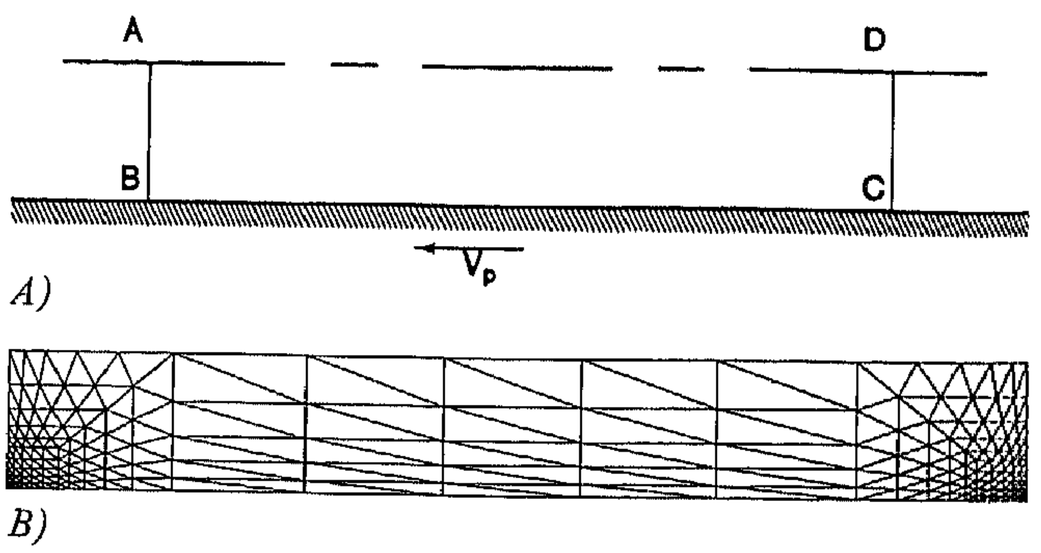

A)

B)

Fig. 11. Flow geometry and mesh

wall is moving at a velocity V_p and D-A is a line of symmetry. This results in the following boundary conditions:

A-B	driving piston	$v_r = 0$	$v_z = 0,$	(5)
B-C	solid wall	$v_r = 0$	$v_z = -v,$	(6)
C-D	driven piston	$v_r = 0$	$v_z = 0,$	(7)
D-A	line of symmetry	$v_r = 0$	$\frac{dv_z}{dr} = 0.$	(8)

Special attention has to be paid to the elements in the corners at points B and C, because here the boundary conditions are contradictory. Therefore a meshrefinement is applied in the corners, a total number of 350 isoparametric triangles proved to be sufficient. In the studies concerning piston driven flow of both, Wagner [1] and Gerrard [2], the singularity problem has been recognized. Gerrard mentions the apparent existence of a gap between piston and wall. He states, however, that the area affected is small, therefore the cornerpoint could be treated as a regular wall point. The problem of the singularity has been approached in two different ways.

The first approach is to remove the singularity by creating a slip condition on the wall. This makes it possible to derive the stress on the cylinder wall. The effect of the slip coefficient on the flow has been investigated by Dussan and Davis [24] and Hocking [14, 25]. They conclude that molecular interactions should be studied and they suggest that the likely outcome of such a study would be equivalent to mathematically replacing the no-slip condition by a slip condition on the boundary. However, because the stress is difficult to measure in the set-up used and because the

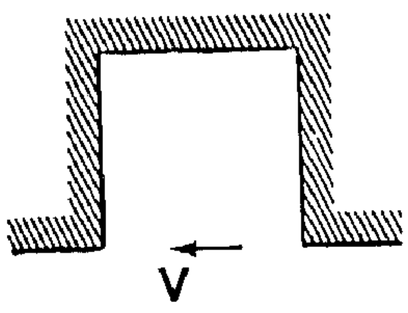

Fig. 12. Flow geometry in a driven cavity

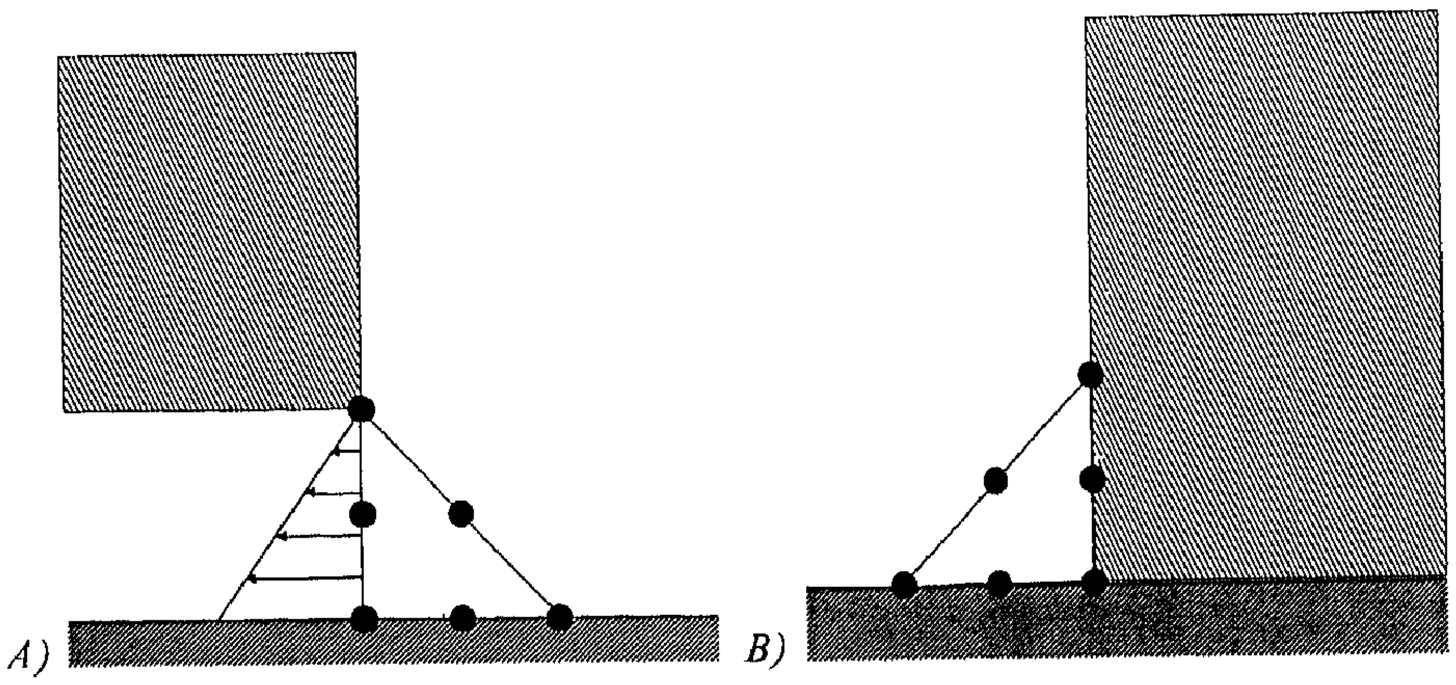

Fig. 13. Boundary conditions at the corner elements
A: driving piston, B: driven piston

postulated slip coefficient has no rational basis, no use is made of a slip condition in this investigation.

The second approach of the problem is to accept the existence of the singularity and consider the boundary conditions in the corner in more detail. In this case a comparison can be made with the extensively studied problem of a wall driven flow in a square cavity, see Fig. 12. The boundary conditions only differ on D-A compare Figs. 11 and 12, and become:

$$v_x = 0 \quad \text{and} \quad v_y = 0. \tag{9}$$

Quite a variety of approximations of the boundary conditions in this problem have been employed by a number of investigators (see e.g. Burggraf [26], Bercovier and Engelman [27], Hughes et al. [28], Nakazawa, Pittman and Zienkiewicz [29]). The different treatments of the boundary conditions can result in significant quantitative differences in the velocity field [28]. Most authors treat the corner-points containing the singularity as a regular wall point. This results in similar boundary conditions in both corner elements. However, the experiments have shown, and it has been recognized, that at the driving piston a leakage flow will occur (Gerrard [2]), while at the driven piston no material is flowing between the piston and the cylinderwall. In consequence of these considerations different boundary conditions are used in the corners as shown in Fig. 13. The influence of these local differences on the global solution must not be underestimated, because the problem is very sensitive to the treatment of the boundary conditions. The main reason for this sensitivity is that not the velocities or velocity-gradients are investigated, but the total deformation, which integrates the velocities over the time. To what extent these approximations influence the solution depends also on the size and shape of the elements, so care must be taken in the interpretation of the results. Introducing a leakage flow at one piston and not at the other is a small violation of the continuity-equation, because material is lost and not replaced again. The error is small (the leakage flow is ± 1 % of the displaced volume) and will not be compensated for.

4.2 Numerical results

Computation of the flow field for Polystyrene at 230 °C with a velocity of 1.2 mm/s yields streamlines as given in Fig. 14. From the velocity-field, it can be concluded that in the middle of the cylinder the two-dimensional flow is fully developed. The fountain flow is most obviously illustrated by the deformation of a material element entering the front region, see Fig. 15. The calculated deformation history of the tracers can be visualized by tracking a large number of points through the velocity field, as shown in Fig. 16. Comparison with the experiments (Fig. 6) shows qualitatively good agreement. The quantitative differences are probably caused by the omission of viscoelastic and transient effects in the calculations. For ABS the computations of the deformation using the power-law model are shown in Fig. 17. Comparison with Fig. 7 of the experiments shows that the deformation is not even described well qualita-

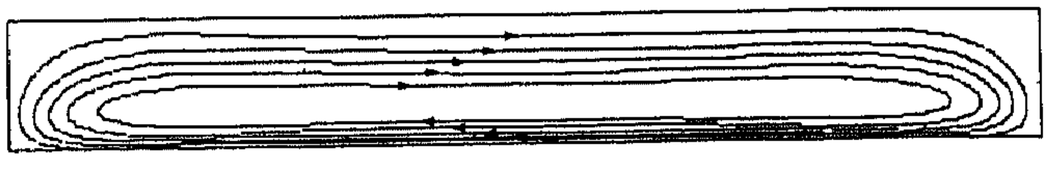

Fig. 14. Streamlines (Carreau model)

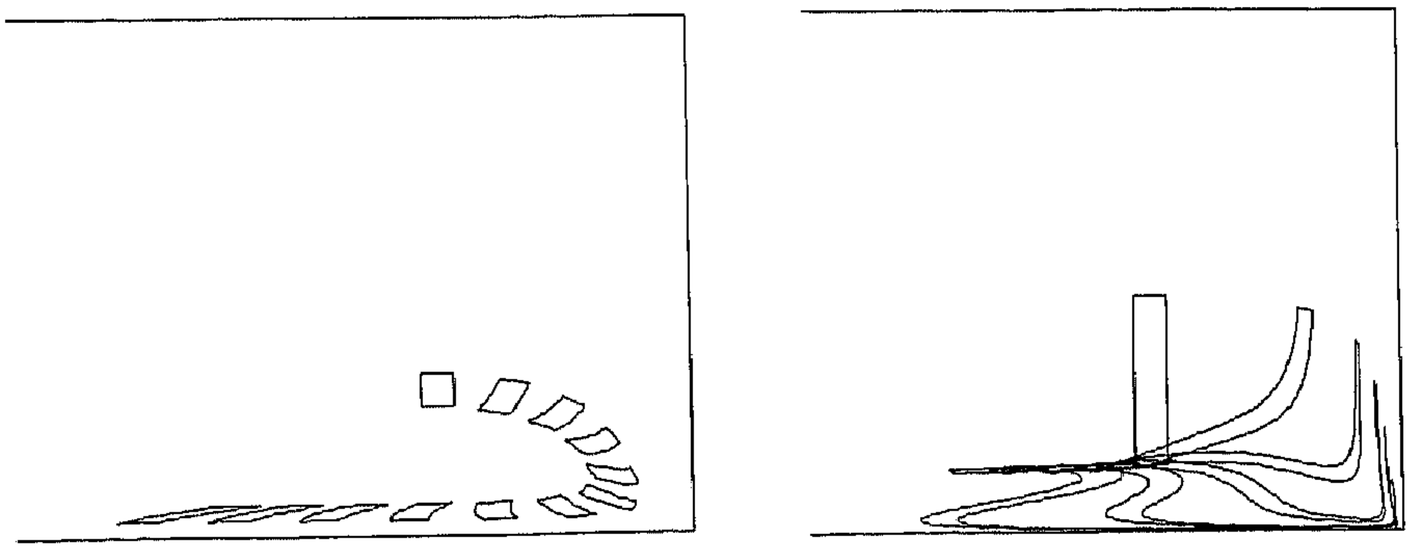

Fig. 15. Calculated deformation on a square (A) and rectangular (B) material element passing through the flow front

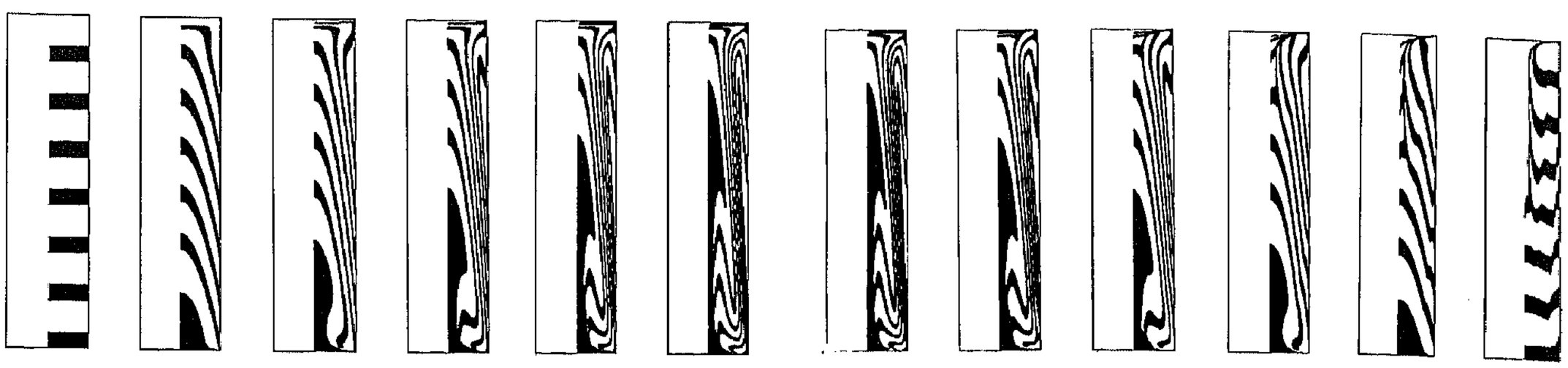

Fig. 16. Calculated deformation using the Carreau model. Displacements are 0, 11, 22, 33, 44 and 55 mm respectively

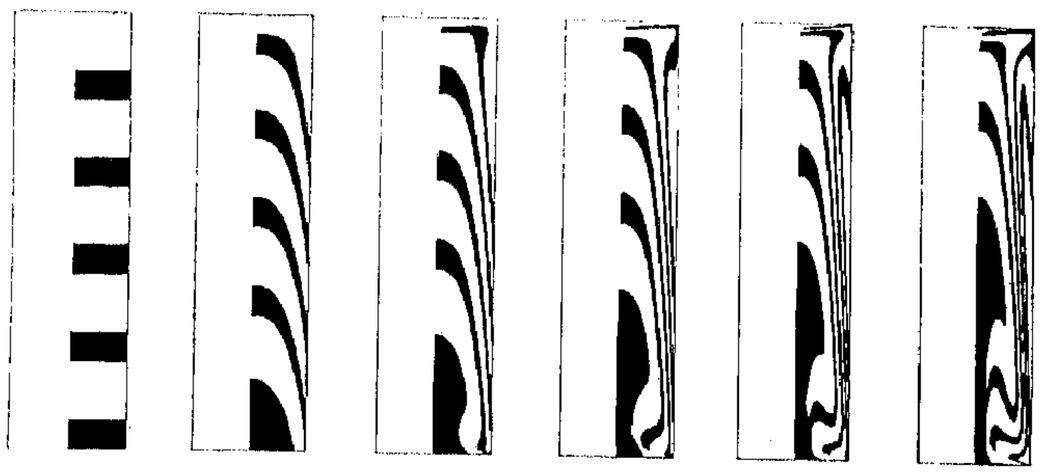

Fig. 17. Calculated deformation using the power law model. Displacements see Fig. 16

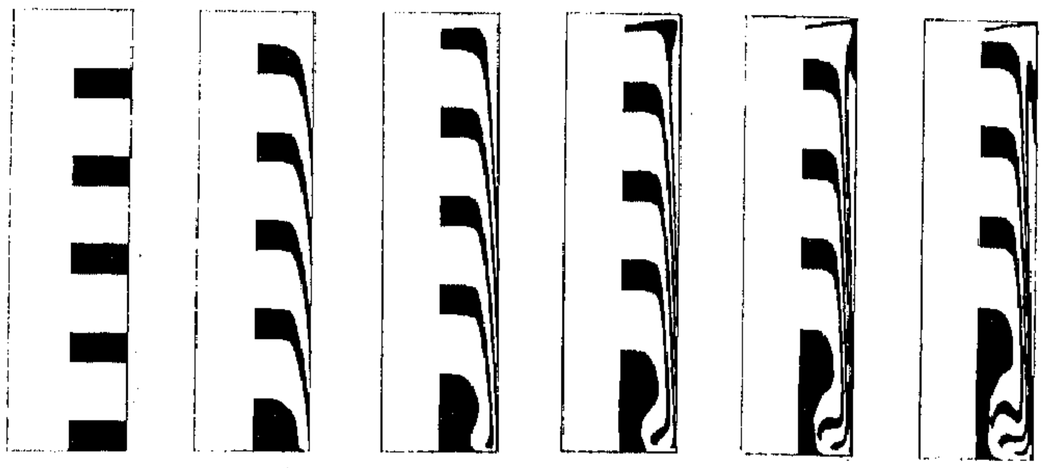

Fig. 18. Calculated deformation using the Bingham model. Displacements see Fig. 16

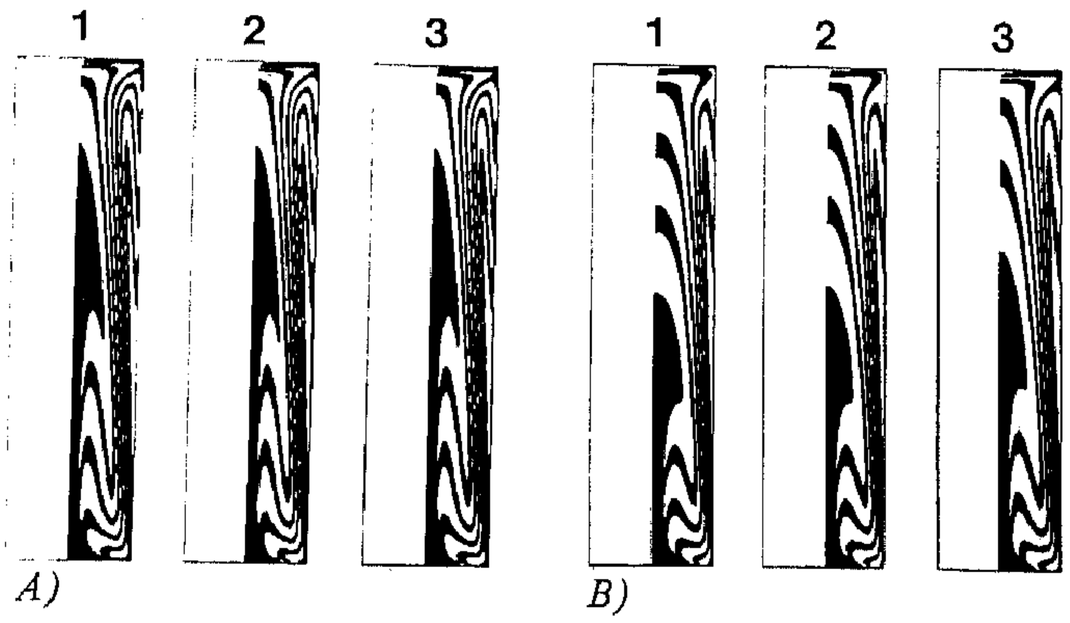

Fig. 19. Calculated effect of velocity and temperature for Polystyrene (Symbols, see Fig. 8)

tively. A probable explanation could be the appearance of a yield stress. It has been shown by Münstedt [30] that a yield stress can occur in rubber modified polymers. This yield stress depends on the size and percentage of the rubber particles. So for ABS another flow model should be used, like the equation derived by Herschel and Bulkey [31, 32]. They combine the yield stress with a power law model:

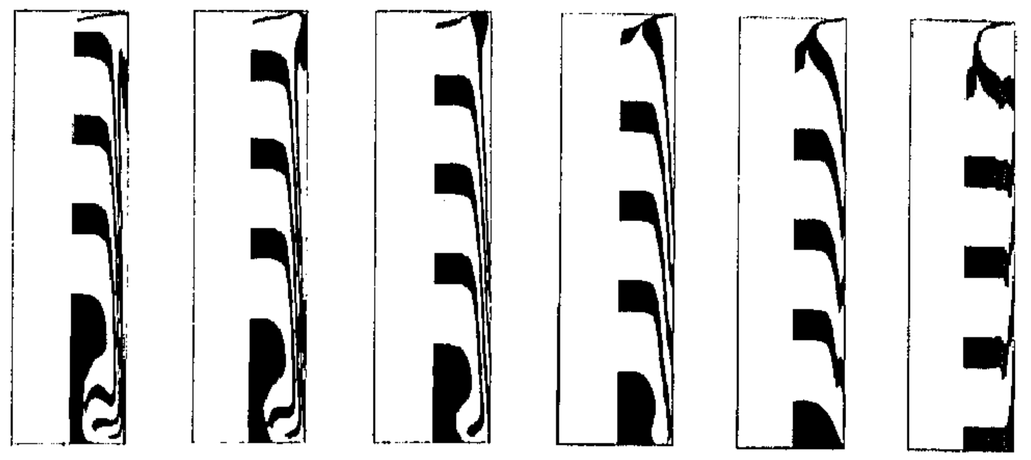

Fig. 20. Simulation of the reverse flow, Carreau model, displacements: 55, 44, 33, 22, 11 and 0 mm respectively

Fig. 21. Simulation of the reverse flow using the Bingham model. Displacements see Fig. 20

$$\eta = \eta_{pl}\dot{\gamma}^{n-1} + \tau_y\dot{\gamma}^{-1}. \tag{10}$$

The finite element program used, does not have this option, therefore some calculations have been performed using the model of a Bingham liquid:

$$\eta = \eta_b\left(1 + \frac{\tau_y}{\eta_b}\dot{\gamma}^{-1}\right). \tag{11}$$

This flow model predicts the qualitative effect of the plug-flow occuring quite well, see Fig. 18. The experiments evaluating the influence of temperature and velocity have also been stimulated, the results for Polystyrene are shown in Fig. 19. The quantitative values are not quite in agreement with the experiments: all calculated deformations are larger, especially at low velocities. These differences can be the result of the transient effect. When comparing the qualitative results of both, calculations and experiments (for Polystyrene Figs. 8 and 19), the calculations predict the trends observed in the experiments quite well. Calculations using the power law model have shown that temperature nor velocity have any influence on the deformation. This also proves that the power law is not the correct flow model to simulate the experiments using ABS, as might have been concluded from the flow curves.

The results of the simulation of the reverse flow are shown in Fig. 20 for the Carreau model (Polystyrene) and Fig. 21 for the Bingham model (ABS). In Fig. 22 the results of the calculations are compared with the experiments for Polystyrene. In general two parts of the plug can be indicated, which do not recover their original layered structure. The first is a part in the centre of the plug, in Fig. 22 between the centreline and line A-B. In the filling stage the material here has entered the fountain flow region. No reversibility results for the middle of the upper two black tracers. This is the material that has closely passed the

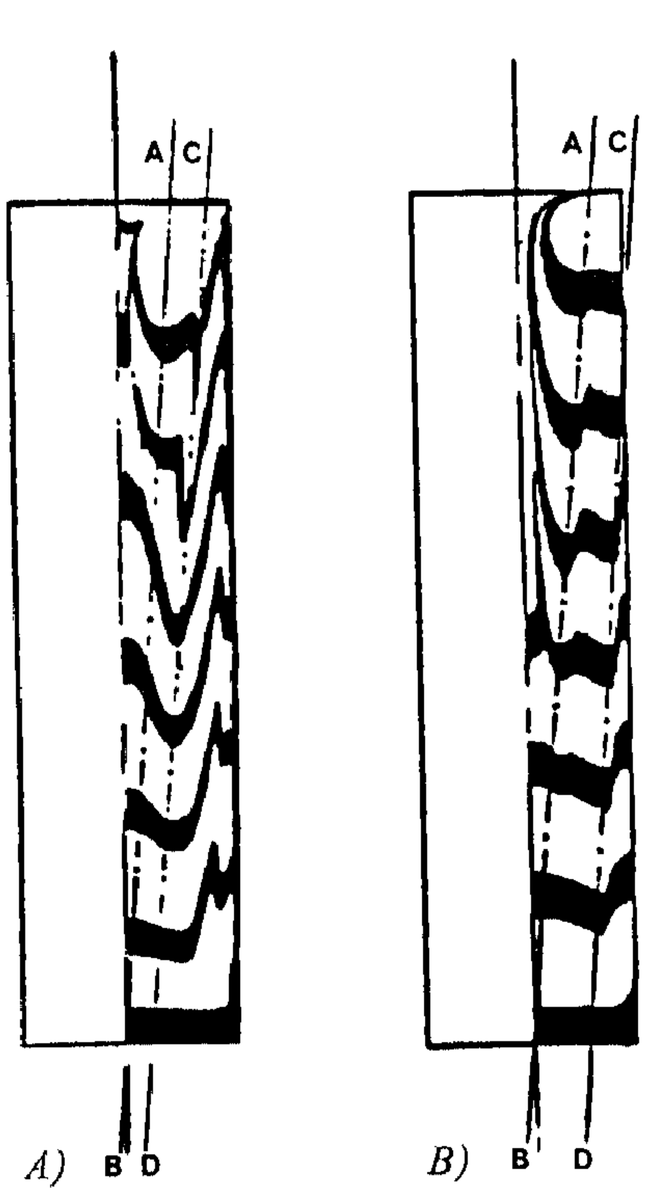

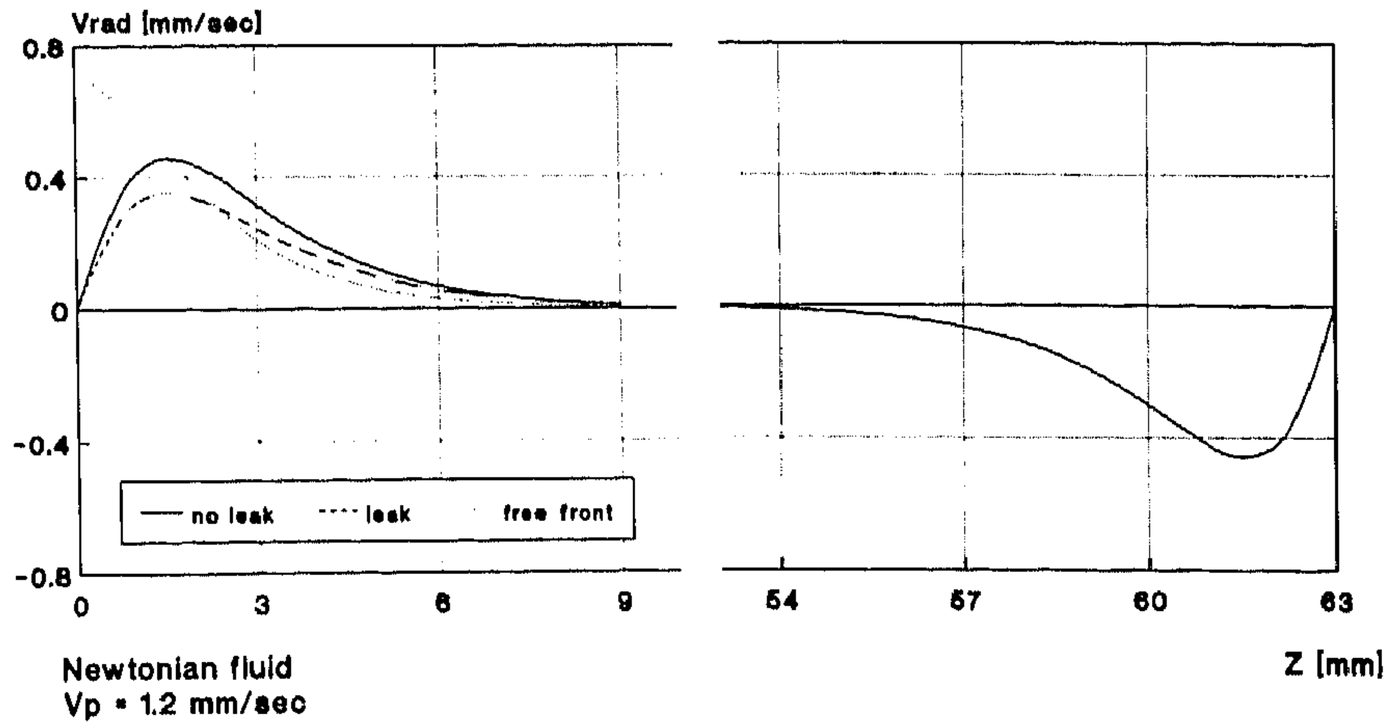

Fig. 23. Radial velocity component on the neutral line, Newtonian fluid, V_p: 1.2 mm/s

Fig. 22. Comparison between experiments (A) and calculations (B) for Polystyrene

contact line of piston and wall in the filling stage and is therefore affected highly by the small leakage flow. The material that has not passed this singularity line shows only a small deviation from the original structure. The second part is the material near the wall, in Fig. 22 between line C-D and the wall. This material has entered the reverse fountain flow. So material that has entered the (reverse) fountain flow region in the filling stage and deformed into the Z or S-shapes, does no regain its original structure after the reverse deformation. This is a result of different velocity fields in these regions, see also Fig. 23. Here the radial velocities on the so-called neutral line in the one dimensional, Newtonian flow ($1/\sqrt{2}$*R) are shown for the simulations with and without a leakage. For ABS these considerations are the same. The quantitative effect, however, is less obvious because a plug flow is developed, with less material entering the (reverse) fountain flow region. The effect of the leakage on the overall solution has also been examined. The magnitude of the leakage flow has been varied by using different boundary conditions or element sizes for the corner element at the driving piston, see Fig. 24. From these data it can be concluded that it should be possible to create boundary conditions in the corner elements which will result in a good qualitative agreement with the experiments.

5 Conclusions

In connection with the investigation of the applicability of an accumulator in a multilayer injection molding technique, an apparatus has been developed to examine the piston driven flow. Furthermore a numerical technique has been used to calculate the flow field and the deformation history of the fluid. Some aspects of the piston driven flow can be compared with the theory of two 'classical' problems, both different on one boundary condition only, these problems are the fountain flow and the driven cavity. Because no account has been taken of transient and viscoelastic effects the quantitative outcomes of the calculations should be interpreted carefully and still will have mainly a qualitative value. Comparison of the model with the experiments leads to a sufficient understanding of the phenomena occuring. It is concluded in both, experiments and modelling, that especially the influence of the discontinuity occuring at the contactline of piston and tubewall should not be underestimated. In fact at low Reynolds numbers this is almost the

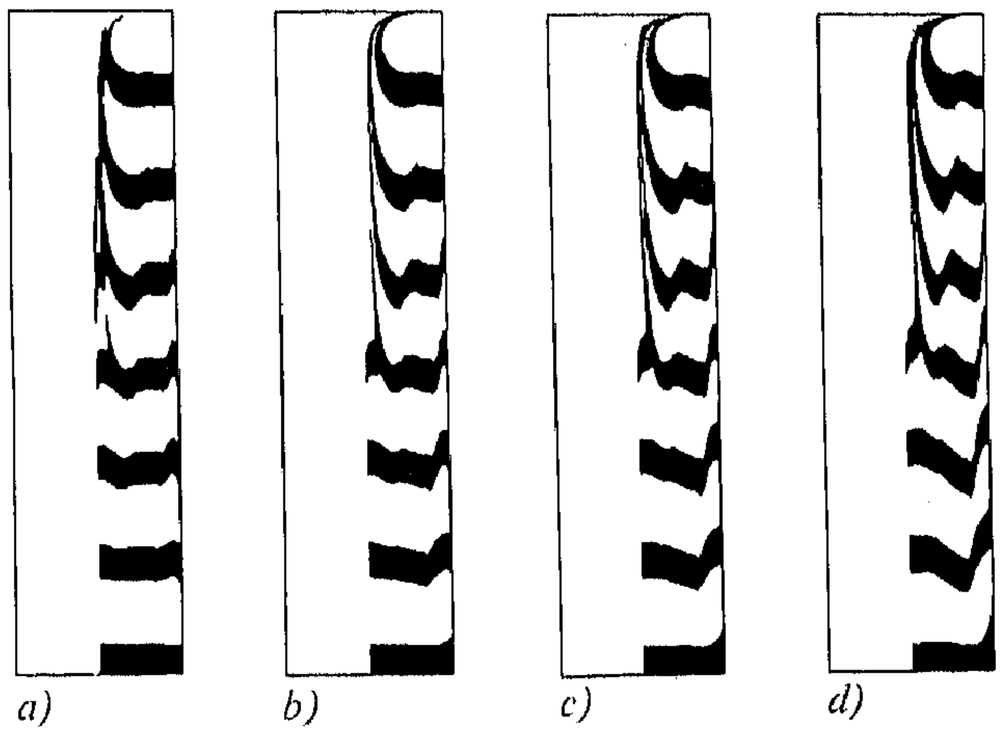

Fig. 24. Calculated effect of different boundary conditions on the end configuration after 55 mm up and down displacement
a, b, c and d correspond to 0, 0.55, 1.1 and 1.65 % leakage respectively

only factor determining the differences in velocity-profile between the flow near a driving and a driven piston. The experiments were performed at low velocities, therefore heating by energy dissipation could be neglected. The singularity has been solved for by introducing a leakage flow in the model in accordance with the observations in the experiments. The global deformation is mainly determined by the rheology of the materials, while the local differences in the deformation seem to be mainly influenced by the discontinuities. If this knowledge is applied to the accumulator, it can be concluded that the piston should closely fit, because of the considerable influence of a leakage. If this leakage flow can not be diminished, other methods of storage should be searched for. When using the piston method, a small L/D ratio can be advised to minimize the effect of the discontinuity. This ratio is limited by the disturbing influence of the divergence of the channel at the inflow. This influence will become dominant at a certain ratio. Recommendations with respect to the rheology of the materials to be used, will depend on the accumulator design and the processing conditions. If low shear rates can be realized both during filling and emptying the accumulator, a material with a yield stress, like the ABS used, will result in a plug flow with minimal deformation in the middle of the tube. Differences in piston speed will cause differences in the total deformation. This can probably be compensated for by the temperature, although this is of little practical meaning. When using materials showing no yield stress, no plug flow will occur. Therefore the influence of the leakage should get even more attention. If the flow curves of these materials are according to the Newtonian or power-law model, thus showing a straight line in the plot of $\log \eta$ versus $\log \dot{\gamma}$, the influence of temperature and velocity will be minimal. Whereas if these flow curves are not straight, like for Polystyrene, the influence of the difference in velocity will be noticable. The direct confrontation of numerical and experimental results yields a tool for the evaluation of small differences in rheological behavior of different materials. Or differences in boundary conditions like slip, compare [32], because not the velocity, velocity gradients, shear stress or pressure drop are measured but the total deformation history of the material under investigation. The integrated velocity profile proves to be a very sensitive measure.

With respect to an evaluation of the application of these results in a multilayer injection molding technology, one should not necessarily be too pessimistic, since the configuration used in this study (see Fig. 4) was deliberately chosen because of its sensitivity for the discontinuities present, since all tracers pass these points. Concentric cylinders with a finite length would have been deformed inside out and backwards without too much disturbance.

References

1 *Wagner, M. H.:* J. Fluid Mech. 72, p. 269 (1975)
2 *Gerrard, J. H.:* J. Fluid Mech. 50, p. 625 (1971)
3 *Hughes, M. D., Gerrard, J. H.:* J. Fluid Mech. 50, p. 645 (1971)
4 *Chien, W. L., Rising, H., Ottino, J. M.:* J. Fluid Mech. 170, p. 355 (1986)
5 *Ottino, J. M., Leong, C. W., Rising, H., Swanson, P. D.:* Nature 333, p. 419 (1988)
6 *Rose, W.:* Nature 191, p. 242 (1961)
7 *White, J. L., Dee, H. B.:* Polym. Eng. Sci. 14, p. 212 (1974)
8 *Dussan, V. E. B.:* AIChE J. 23, p. 131 (1977)
9 *Brown, C. E., Jones, T. J., Neustadter, E. L.:* J. Colloid Interf. Sci. 76, p. 582 (1980)
10 *Schmidt, L. R.:* Polym. Eng. Sci. 14, p. 797 (1974)
11 *Cogos, C. G., Huang, C., Schmidt, L. R.:* Polym. Eng. Sci. 26, p. 1457 (1986)
12 *Coyle, D. J., Blake, J. W., Macosko, C. W.:* AIChE J. 33, p. 1168 (1987)
13 *Bhattacharji, S., Savic, P.:* Proc. 1965 Heat Transf. Fluid Mech. Inst. p. 248 (1965)
14 *Hocking, L. M.:* J. Fluid Mech. 79, p. 209 (1977)
15 *Lafleur, P. G., Kamal, M. R.:* Polym. Eng. Sci. 26, p. 92 (1986)
16 *Kamal, M. R., Lafleur, P. G.:* Polym. Eng. Sci. 26, p. 103 (1986)
17 *Kamal, M. R., Lafleur, P. G., Ryan, M. E.:* Polym. Eng. Sci. 26, p. 190 (1986)
18 *Lowndes, J.:* J. Fluid Mech. 101, p. 631 (1980)
19 *Behrens, R. A., Crochet, M. J., Denson, C. D., Metzner, A. B.:* AIChE J. 33, p. 1178 (1987)
20 *Mavridis, H., Hrymak, A. N., Vlachopoulos, J.:* J. Rheol. 32, p. 639 (1988)
21 *Mavridis, H., Hrymak, A. N., Vlachopoulos, J.:* Polym. Eng. Sci. 26, p. 449 (1988)
22 *Beris, A. N.:* J. Rheol. 31, p. 121 (1987)
23 *Carey, G. F., Krishnan, R.:* Finite elements in fluids 6, p. 189 (1985)
24 *Dussan, V. E. B., Davis, J.:* J. Fluid Mech. 65, p. 71 (1974)
25 *Hocking, L. M.:* J. Fluid Mech. 76, p. 801 (1979)
26 *Burggraf, O. R.:* J. Fluid Mech. 24, p. 113 (1966)
27 *Bercovier, M., Engleman, M.:* J. Comp. Phys. 30, p. 181 (1979)
28 *Hughes, T. J. R., Liu, W. K., Brooks, A.:* J. Comp. Phys. 30, p. 1 (1979)
29 *Nakazawa, S., Pittman, J. F. T., Zienkiewicz, O. C.: Finite Elements in Fluids* 4, p. 251 (1982)
30 *Münstedt, H.:* Polym. Eng. Sci. 21, p. 259 (1981)
31 *Ottino, J. M.:* The Kinematics of Mixing: Stretching, Chaos and Transport. Cambridge University Press Cambridge 1989
32 *Uhland, E.:* Rheol. Acta 18, p. 1–24 (1979), p. 15, and 30 to 39 (1976)

Date of acceptance: February 4, 1990